Naval Research Laboratory
Washington, DC 20375-5320

NRL/MR/6750--05-8902

On Collisionless Energy Absorption in Plasmas: A Theoretical and Experimental Investigation in Spherical Geometry

David N. Walker
Richard F. Fernsler
David D. Blackwell
William E. Amatucci
Sarah J. Messer, NRL-NRC Postdoctoral Associate

Charged Particle Physics Branch
Plasma Physics Division

September 28, 2005

Approved for public release; distribution is unlimited.

REPORT DOCUMENTATION PAGE

Form Approved
OMB No. 0704-0188

Public reporting burden for this collection of information is estimated to average 1 hour per response, including the time for reviewing instructions, searching existing data sources, gathering and maintaining the data needed, and completing and reviewing this collection of information. Send comments regarding this burden estimate or any other aspect of this collection of information, including suggestions for reducing this burden to Department of Defense, Washington Headquarters Services, Directorate for Information Operations and Reports (0704-0188), 1215 Jefferson Davis Highway, Suite 1204, Arlington, VA 22202-4302. Respondents should be aware that notwithstanding any other provision of law, no person shall be subject to any penalty for failing to comply with a collection of information if it does not display a currently valid OMB control number. **PLEASE DO NOT RETURN YOUR FORM TO THE ABOVE ADDRESS.**

1. REPORT DATE *(DD-MM-YYYY)*	2. REPORT TYPE	3. DATES COVERED *(From - To)*
28-09-2005	Memorandum Report	

4. TITLE AND SUBTITLE

On Collisionless Energy Absorption in Plasmas: A Theoretical and Experimental Investigation in Spherical Geometry

5a. CONTRACT NUMBER

5b. GRANT NUMBER

5c. PROGRAM ELEMENT NUMBER

6. AUTHOR(S)

David N. Walker, Richard F. Fernsler, David D. Blackwell,
William E. Amatucci, and Sarah J. Messer*

5d. PROJECT NUMBER
67-3419-15

5e. TASK NUMBER

5f. WORK UNIT NUMBER

7. PERFORMING ORGANIZATION NAME(S) AND ADDRESS(ES)

Naval Research Laboratory, Code 6755
4555 Overlook Avenue, SW
Washington, DC 20375-5320

8. PERFORMING ORGANIZATION REPORT NUMBER

NRL/MR/6750--05-8902

9. SPONSORING / MONITORING AGENCY NAME(S) AND ADDRESS(ES)

Office of Naval Research
800 North Quincy Street
Arlington, VA 22217

10. SPONSOR / MONITOR'S ACRONYM(S)

ONR

11. SPONSOR / MONITOR'S REPORT NUMBER(S)

12. DISTRIBUTION / AVAILABILITY STATEMENT

Approved for public release; distribution is unlimited.

13. SUPPLEMENTARY NOTES

*NRL-NRC Postdoctoral Associate

14. ABSTRACT

We are investigating the RF impedance characteristics of a small spherical probe immersed in a laboratory plasma. The experimental facility is the large Space Physics Simulation Chamber at the Naval Research Laboratory. The data taken are from network analyzer measurements of the reflection coefficient obtained when applying a low-level RF signal to the probe, which is either near-floating potential or negatively DC-biased in a low-pressure plasma. As is well known, sheaths form around objects placed inside plasmas. The electron density is smaller inside the sheath, and the reduction in density alters the plasma impedance. Surprisingly, the impedance becomes "resistive," even though the plasma is effectively collisionless, at frequencies below the bulk-plasma frequency, thus leading to collisionless energy absorption.

15. SUBJECT TERMS

Plasma; Collisionless absorption; Laboratory experiments; Plasma-sheath formation

16. SECURITY CLASSIFICATION OF:			17. LIMITATION OF ABSTRACT	18. NUMBER OF PAGES	19a. NAME OF RESPONSIBLE PERSON
a. REPORT	b. ABSTRACT	c. THIS PAGE			David N. Walker
Unclassified	Unclassified	Unclassified	UL	34	19b. TELEPHONE NUMBER *(include area code)* (202) 767-2248

TABLE OF CONTENTS

On Collisionless Energy Absorption in Plasmas: A Theoretical and Experimental Investigation in Spherical Geometry*

D. N. Walker, R.F. Fernsler, D.D. Blackwell, W.E. Amatucci, and S.J. Messer[1]

Plasma Physics Division, Naval Research Laboratory, Washington, DC 20375,
[1] NRL-NRC Postdoctoral Associate * Work supported by ONR

I. Abstract

We are investigating the RF impedance characteristics of a small spherical probe immersed in a laboratory plasma. The experimental facility is the large Space Physics Simulation Chamber at the Naval Research Laboratory. The data taken are from network analyzer measurements of the reflection coefficient obtained when applying a low level RF signal to the probe which is either near floating potential or negatively DC-biased in a low pressure plasma. As is well known, sheaths form around objects placed inside plasmas. The electron density is smaller inside the sheath, and the reduction in density alters the plasma impedance. Surprisingly, the impedance becomes "resistive", even though the plasma is effectively collisionless, at frequencies below the bulk plasma frequency, thus leading to collisionless energy absorption. This behavior comes directly from solving Maxwell's equations together with cold fluid equations, and the solutions obtained indicate that the plasma resistance is inversely proportional to the plasma density gradient evaluated at the location where the plasma frequency is equal to the applied frequency. The resistance is appreciable, however, only if the sheath is nearly as thick as the sphere, and thus for our plasmas the sphere must be small in order that resistive effects be evident. Applying a supplemental, negative DC bias to the sphere thickens the sheath and thereby raises its resistance. Doing so helps increase the power transferred to the plasma. Much of the earlier work in this area of collisionless resistance concentrated primarily on planar probes as opposed to the present work which is concerned with spheres. Interpreting the results is simpler for a sphere and the results obtained agree well with theory as described. For comparison to the theory we use only the S_{11} parameter outputs (or reflection coefficients) of the network analyzer in the experimental series. Significant energy absorption is observed at frequencies generally near one-half the plasma frequency. One result of this is that the most efficient transfer of power to the plasma occurs not unexpectedly when there is impedance matching between input impedance and output (collisionless) impedance. This paper is an exposition of these ideas along with data results and a comparison to theory for the spherical probe which to our knowledge has not been published in this form.

Manuscript approved August 31, 2005.

II. Introduction

The use of RF impedance probes to measure plasma parameters is a well-established experimental method investigated early on in both the laboratory[1,2] and in the space plasma environment nearly a half-century ago[3]. More recently in the laboratory there have been continuing experimental and theoretical studies[4,5] of plasma-sheath resonance phenomena. In addition to providing electron density, recent work[4] concentrates on improving low pressure plasma processing by providing a novel operation mode for parallel plate reactors. Another study[5] concentrates on measurement of plasma density, temperature and collision frequency in a laboratory plasma in the presence of collision frequencies on the order of or larger than the plasma frequency. In space, various forms of plasma frequency-based resonant probes are regularly used to investigate electron density and temperature from satellites and often in night time rocket investigations of mesospheric or ionospheric phenomena[6,7]. Theoretical treatment and the analysis of data from impedance probes and antennas of various shapes and sizes is to be found in numerous studies.[8,9,10] There is a body of early theoretical and experimental work related to the phenomenon of RF resonance both above and below the plasma frequency.[11,12,13]

The investigation of collisionless resistance associated with resonance phenomena that is thought to arise due to plasma inhomogeneity, may be said to originate with the work of Tonks[14]. However the problem did not receive further attention until Herlofson[15], trying to account for resonant scattering observed in connection with ionized meteor trails, was the first to introduce the idea of an effective collision frequency associated with density gradients. The phenomenon associated with this effective collision frequency was named the *Herlofson paradaox* and was not treated until some years later[16] when the physically appealing explanation arose that a plasma with a density gradient may be viewed as a continuous distribution of uncoupled oscillators, each oscillator representative of the plasma frequency at a given location. In this idea, the driving energy is dispersed as a transient response into differing plasma frequencies and therefore it is not sufficient to consider only one Fourier component in the analysis. In a rigorous mathematical treatment[17] the problem of a conducting sphere immersed in a homogeneous plasma was analyzed. Using the Boltzmann-Vlasov equations along with Maxwell's equations this work was able to arrive at both the impedance and the electric field under an assumption of a realistic sheath potential distribution. The final results include a real part to the impedance which is dependent upon neutral collisions even for the case in which the sheath is assumed to be vacuum and the plasma is homogeneous. In other early resonance probe work[18] related to spherical probes, the justification for resonance conditions also required electron-neutral collisions. Neither work treats in any detail ideas of collisionless absorption. Perhaps the first exhaustive theoretical treatment aimed specifically at collisionless absorption[19] obtains an expression for the collisionless resistance by comparing total energy input to a driven parallel plate capacitor to that absorbed (This article contains detailed references to early investigations of the phenomenon). In this work, the impedance of a plasma contained between two parallel plates and possessing a symmetric density gradient results in a contour integral for which there is a non-zero, and real, positive residue. It is this residue which was treated properly in this work and is responsible for the absorption. Researchers during this time were active in uncovering still further experimental and theoretical bases for the observations in general investigations of resonance probes In more recent work[4,22,23] the

phenomenon is treated in a in a series of experiments accompanied by theory.

The basis of these measurements lies in the observation that the impedance properties associated with an antenna or probe are altered by the presence of a plasma and from these alterations plasma characteristics can be determined. In vacuum, for example, there is no significant electromagnetic radiation from a loop antenna until the wavelength of the driving signal is on the order of the loop circumference. Antenna size, along with its shape, with respect to frequency influences power requirements necessary to produce detectable electromagnetic radiation. In this case, a radiation resistance is defined by the ratio of input power to the square of the antenna current. When power is being radiated and there is insignificant internal antenna resistance this ratio allows a definition of a "resistance" and hence a radiated power. A device measuring the ratio of input power to reflected power from such an antenna would see this ratio drop to less than one assuming there is no impedance mismatch between the signal generator and the antenna with its associated cabling. In the presence of a plasma, however, there is an additional means to transfer energy from the antenna through internal plasma currents which can arise due to the presence of antenna current itself and the interaction of the antenna with the plasma which occurs through the sheath. In one work, for example, it was shown[21] that very small radiated power emitted from an antenna in vacuum is increased through plasma-sheath coupling to the plasma by a factor of ~400 when immersed in a plasma. Measuring antenna impedance when the antenna is placed inside a plasma then provides a method of studying the plasma fluctuations which are excited and from this study to infer plasma characteristics.

Langmuir oscillations in a cold plasma occur at the plasma frequency and are expressible in terms of an impedance which is only capacitive and inductive. However, if there are collisional processes associated with the plasma currents the impedance acquires a resistive component. And so it is natural to associate this energy transfer also with an effective antenna resistance in the same manner as is done in the classical definition of radiation resistance cited above. At first glance in a cold, collisionless, unmagnetized plasma there would appear to be no means of dissipating the driving energy to extract useful energy (again assuming negligible antenna resistance) since there is no resistive term and the capacitive and inductive responses are adiabatic. Nevertheless, energy absorption often occurs in such plasmas for various antenna shapes. Central to this absorption is the formation of a plasma sheath around the antenna. It has long been known that energy dissipation can occur at frequencies lower than the plasma frequency in collisionless plasmas at frequencies characterized as the sheath-plasma resonance. [1,4, 8,11,13, 16,17,18,22, 23]

To more accurately predict the result of applying an AC signal to a probe immersed in a collisionless plasma, the simple hydrodynamic approach was replaced by a solution of the Vlasov equation[17,18] with plasma resonances related to gradients in electron density as already noted. In the simplest model of the antenna immersed in a plasma the sheaths are treated as vacuum capacitors, the plasma impedance arises as a series combination of inductor-resistor in parallel with a capacitor, and the solutions for net impedance appear as parallel and series resonant solutions.[24,25] For the collisionless plasma without sheaths the impedance is purely reactive and results in no energy absorption. With sheaths included there arises an energy deposition which is a function of the density

profile in the sheath. Resonance power transfer which occurs results from the fact that at resonance the reactance of the antenna-plasma system is near zero and therefore the impedance becomes all resistive. The resonances are "Landau-type" resistive components arising in cold, collisionless plasmas. Toward a more physical insight into these resonances, it was pointed out in a brief communication[28] that a network of a large number of resonating circuits with differing time constants exhibits resistance properties in a thermodynamic sense as a transient response. From a physical point of view this represents a different form of energy dispersal than in the collisional case. Since there is a multitude of ways that the energy can be dispersed, the process is thermodynamically irreversible in the sense that it is highly unlikely that any "reflected" energy would be returned in its original form.

Another mechanism cited for energy absorption when driving a probe with an RF signal is the phenomenon of stochastic heating.[29,30] The idea inherent in this power transfer scheme is that there is a sheath oscillation produced by the driving signal from which electrons can be reflected in the case of a sufficiently high voltage sheath. On average this can be shown to result in a power transfer which is proportional to the difference in electron and sheath velocities in addition to the electron distribution function.[24] The oscillating voltage levels we apply to the probe in the experiment are small compared to the floating potential or any DC bias potentials and are considered a perturbation. In this case, it appears that the idea of a sheath oscillation contributing to power loss is remote. Nevertheless we consider power transfer below for varying levels of the applied signal voltage.

Our aim in the brief work here is to derive an approximation to the expected collisionless resistance for a small spherical probe in a vacuum chamber and to compare these predictions with experimental results which indicate energy absorption at frequencies less than the plasma frequency. The general result is not specific with respect to the assumed sheath electron density profile but we calculate results for a model of the collisionless sheath and compare these results to measurements of the network analyzer . The measurement method uses only the ratio of reflected to total power for a small Aluminum sphere inserted into a plasma, biased either not at all or into ion saturation, and driven by a small RF signal. In other papers[25,25a] we have used a basic circuit model in order to understand impedance observations obtained from the network analyzer for the driven sphere. In addition those papers shows how one can infer both plasma density and sheath thickness from the measurements. In this paper, we concentrate only on observations of energy absorption.

III. Experimental Configuration

The experimental facility consists of a large-volume cylindrical chamber, in addition to a smaller high-magnetic field chamber which is separated from the main volume by a large gate valve. The series here was performed in the large chamber whose radius and length are (2m x 5m). Typical densities of the argon plasma for the series vary from 10^7 to 10^9 cm^{-3}. Electron temperature is near 0.5 eV and since the chamber is operated at pressures near 3×10^{-4} Torr, $\nu_{en} \sim 6 \times 10^5$ s^{-1} and ω_{p0}, the plasma frequency, is typically 9×10^8 s^{-1}. Neutrals and therefore ions are at room temperature. The plasma is created by a tungsten filament source located at one end of the large chamber and covering a large portion of the inner end-plate surface area. It is maintained by a low-level axial magnetic field on the order of 2-3 Gauss provided by 5 coils aligned axially in a Helmholtz configuration and so the

plasma is not magnetized to the level that Larmor orbits become important which is demonstrated below. Electron density and temperature measurements are made with a heated Langmuir probe. Further details of the experimental configuration and the general laboratory setup are to be found elsewhere.[26,27]

The small Aluminum sphere of 0.95 cm radius is connected to an HP8735D Network Analyzer through 50 Ω coaxial cable. The cabling is 1/4" semi-rigid coax whose outer jacket and dielectric are removed at a short section at the tip to allow the center conductor to be inserted into the sphere for mounting. This arrangement is described in an earlier paper[25].

The primary measurement of interest for this work is the network analyzer measurement of reflected power which is related to plasma impedance through,

$$\Gamma = \frac{Z - Z_0}{Z + Z_0} \tag{1}$$

where $|\Gamma|^2$, is the ratio of reflected-to-total power. Z is the external impedance and the internal impedance of the Network Analyzer, Z_0, is 50 Ω and the additional impedance from the cabling and shaft can be compensated by proper calibration of the instrument when connected either to another 50 Ω resistor or when calibrated as an open circuit. A significant advantage of this technique is that these procedures essentially allow the removal of the effects associated with the transmission line.

IV. Theory

a. Impedance

We use Maxwell's equations directly along with the electron momentum equation to obtain an expression for the impedance. From Gauss' law,

$$\nabla \cdot \boldsymbol{E} = 4\pi\rho \ , \tag{2}$$

along with the continuity equation,

$$\frac{\partial}{\partial t}\rho + \nabla \cdot \boldsymbol{j} = 0, \tag{3}$$

we obtain,

$$\nabla\cdot(\frac{\partial \boldsymbol{E}}{\partial t}+4\pi \boldsymbol{j})=0. \tag{4}$$

For a sphere the field and current are purely radial, so that,

$$\frac{1}{r^2}\frac{\partial}{\partial r}[r^2(4\pi j+\frac{\partial E}{\partial t})]\equiv 0. \tag{5}$$

From the form of this equation we recognize that the sum of conduction and displacement currents leaving the sphere is constant in space and must be the same as the total current $I_0(t)$. This allows,

$$4\pi \boldsymbol{j}+\frac{\partial \boldsymbol{E}}{\partial t}\equiv\frac{I_0(t)}{r^2}. \tag{6}$$

If we further assume that electrons, being the lightest species, carry all the current, that they are cold, and that the wave amplitude is small, the electron momentum equation reduces to,

$$\frac{\partial \boldsymbol{j}}{\partial t} = \frac{e^2 E n_e}{m}-\nu \boldsymbol{j}. \tag{7}$$

where ν is the electron collision frequency. [The important point here is that we are assuming cold electrons and $\omega >> /V_e\cdot\nabla/$. This is true as long as the RF amplitude is not too high. For example, in the experiments the sheath width $s > \lambda_D$ by assumption and $Ve\cdot\nabla$ can be dropped as long as $V_e<<(T_e/m)^{1/2}$ as is almost always the case.] Then if j and E vary as $e^{i\omega t}$ the current density is,

$$\boldsymbol{j}=\frac{e^2 n_e}{m(\nu+i\omega)}\boldsymbol{E}=\frac{\omega_{pe}^2}{4\pi(\nu+i\omega)}\boldsymbol{E}\ , \tag{8}$$

so that we may finally write the expression for $E(r,t)$ as,

$$\boldsymbol{E}(r,t)=\frac{I_0(t)}{r^2[i\omega+\frac{\omega_{pe}^2}{(\nu+i\omega)}]} = \frac{I_0(t)}{r^2}\frac{\nu+i\omega}{(\omega_{pe}^2-\omega^2)+i\omega\nu}. \tag{9}$$

From this form the impedance is obtained,

$$Z=\frac{V_0}{I_0}=\frac{1}{I_0}\int_{R_1}^{\infty} dr\ E(r,t) = \int_{R_1}^{\infty}\frac{dr}{r^2}\frac{\nu+i\omega}{(\omega_{pe}^2-\omega^2)+i\omega\nu} \tag{10}$$

where V_0 is the voltage across the plasma. We point out that this expression was derived independently of any assumption regarding an electron density profile. To include a sheath the integral limits will change to accommodate the sheath density profile as separate from that of the bulk plasma. Although this expression for Z was gotten by a straightforward application of Maxwell's equations, models for probe plasma interactions often rely on elementary capacitance arguments. For completeness, in Appendix I we derive again Eqn (10) using an analogy to concentric spheres and allowing for an electron density gradient in the region where energy absorption occurs.

The evaluation of integrals of the type seen in Eqn (10) has been the subject of numerous articles over the years outlined in the Introduction. Simply stated, there is a pole in the integrand generated by the inhomogeneity in plasma density which forces an evaluation of the integral as a contour integral in the upper-half complex plane circling half the pole. (This pole can be seen from setting $\nu = 0$ and noting that the integrand has a singularity at $\omega_{pe} = \omega$. If then $\omega_{pe} = \omega_{pe}(r)$ the integral will have a singularity at those locations, r, for which $\omega = \omega_{pe}(r)$). In early attempts[14] the contribution from the pole was ignored and the result of the integration is purely imaginary. The complete result of this integration however includes both the imaginary contribution which arises from the principal value of the integral in addition to the residue from the poles which is real and is responsible for energy absorption and depends ultimately on the geometry. We may evaluate this integral by a change of variable. Assuming $\nu = 0$, we may rewrite the impedance as,

$$Z=\int_{r_1}^{\infty}\frac{dr}{r^2}\frac{i\omega}{(\omega_{pe}^2-\omega^2)}=i\omega\int_{\omega_{p1}^2}^{\omega_{ps}^2} d(\omega_{pe}^2)\left[\frac{d\omega_{pe}^2}{dr}\right]^{-1}\frac{1}{r^2(\omega_{pe}^2)(\omega_{pe}^2-\omega^2)} \tag{11}$$

which results in,

$$Z\equiv i\omega P+\frac{\pi\omega}{r_r^2}\left[\frac{d\omega_{pe}^2}{dr}\right]^{-1}\Big|_{r=r_r}. \tag{12}$$

In Eqn (11), ω_{ps} is the final bulk electron density and ω_{p1} is the density at the probe surface usually taken to be zero. ω_{pe} is the electron plasma frequency associated with position r, ω is the applied RF signal, and r_r is a resonant position. Included in Eqn (12) are the principal value P contribution to the integral, which is the reactive part of the impedance, and the last term, which is the resistance residue

from the pole at r_r. The resistance exists only if $r_l < r_r < r_s$, where r_l is the sphere radius and r_s is the sheath or within the sheath where $s = r_s - r_l$. Beyond $r = r_s$, the density is assumed constant. Effectively Eqn (12) exhibits a varying resistance as a function of the frequency, ω, of the applied signal and hence an avenue for energy deposition as a function of frequency. We stress at this point then that the collisionless resistance calculated arises not from a bulk plasma density gradient but from a density gradient in the sheath at the probe itself. That the plasma inhomogeneity in the sheath can be responsible for collisionless energy absorption is not new. Many studies of antenna radiation in plasmas[18,32] conclude that energy is absorbed in inhomogeneous ion sheaths around the antenna when trying to radiate at a frequency which matches a localized plasma frequency in the sheath.

Eqn (8) indicates that a collisionless plasma is resistive only if $\omega_l < \omega < \omega_{max}$ and that the RF resistance is given by

$$R(\omega) \equiv Re(Z_{rf}) = \frac{2\pi^2}{A_r}\left[\frac{d\omega_{pe}}{dr}\right]^{-1}\Big|_{r=r_r} \qquad (13)$$

Here A_r is just $4\pi r_r^2$, the surface area at the resonant radius, r_r. As ω increases, the resonant area increases while $d\omega_{pe}/dr$ decreases. The resistance peaks at a frequency ω_{pk} lying between ω_l and ω_{max}. If the sheath is much thinner than r_l the resistance peaks near the transition from the sheath to the presheath in which case $\omega_{pk} \approx (0.6)^{1/2}\,\omega_{max}$. However, for a thick sheath the resistance peaks within the sheath (closer to the sphere), in which case $\omega_{pk} \leq 0.5\,\omega_{max}$.

To estimate the reactive impedance, we observe that the integrand for P changes sign at r_r. If we assume the contributions from the two regions on either side of r_r are small or cancel, the reactive impedance is given by

$$Z_i = i\omega P \cong \frac{i\omega}{r_b(\omega_{max}^2 - \omega^2)} \qquad (14)$$

In the experiments, the sphere radius is $r_l = 0.95$ cm while the sheath thickness typically satisfied $s \geq 4\lambda_D \sim 0.2$ cm. The presheath was far thicker yet (about 15 cm at 0.3 Torr), and thus the highest resistance is expected to occur when $\omega \approx 0.8\,\omega_{max}$. The peak resistance can reach 20 kΩ or so, but only over a narrow range in frequency. Applying a negative DC bias to the sphere can lower the peak resistance by increasing s.

b. A sheath model

To evaluate $d\omega_p/dr$ inside the sheath, we assume(i) the sphere is capacitively coupled and (ii) the sheath is collisionless. With these assumptions we develop the following model for the sheath density profile. For a collisionless sheath containing no sources or sinks, energy conservation limits (inward) dc ion flow velocity to,

$$u_+(r)=c_s[1-\frac{2e\phi}{T_e}]^{\frac{1}{2}} \tag{15}$$

while flux conservation dictates that

$$n_+(r)= \frac{c_s}{u_+(r)}[\frac{r_s}{r}]^2 n_s= n_+(s)[1-\frac{2e\phi}{T_e}]^{-\frac{1}{2}}[\frac{r_s}{r}]^2 \tag{16}$$

Here n_+ is ion density, T_e is the electron temperature, $c_s = (T_e/M)^{1/2}$ is the Bohm speed, M is the ion mass, $n_+(r_s)$ is the density at the sheath edge r_s, and $\phi \leq 0$ is the electrostatic potential relative to its value at r_s.

For electrons, we can use the Boltzmann approximation,

$$n_e(r)= n_e(r_s)\exp[\frac{e\phi(r)}{T_e}] \tag{17}$$

and assume current neutrality,

$$n_e(r)u_e(r)= n_+(r_s)u_+(r) \tag{18}$$

because the sphere is capacitively coupled. Kinetic theory indicates that the electron velocity at the sphere radius r_0 satisfies,

$$u_e(r_1)=[\frac{T_e}{2\pi m}]^{\frac{1}{2}} \tag{19}$$

where m<<M is the electron mass. If we also assume quasineutrality at the sheath edge,

$$n_e(r_s) = n_+(r_s) = n_s \tag{20}$$

the electron density at the sphere ($r = r_1$) is given by,

$$n_e(r_1) = n_s[\frac{r_s}{r}]^2[\frac{2\pi m}{M}]^{\frac{1}{2}} = n_+(r_1)[(\frac{2\pi m}{M})(1-\frac{2e\phi(r_1)}{T_e})]^{\frac{1}{2}} \tag{21}$$

Poisson's equation then closes the model:

$$\frac{1}{r^2}\frac{d}{dr}[r^2\frac{d\phi}{dr}] = 4\pi e[n_e(r) - n_+(r)] \tag{22}$$

Using Eqns (16) and (17), Eqn (22) may be rewritten as,

$$\frac{1}{r^2}\frac{d}{dr}[r^2\frac{d\phi}{dr}] = 4\pi e n_s[r^2\exp(\frac{e\phi}{T_e}) - r_s^2(1-\frac{2e\phi}{T_e})^{-\frac{1}{2}}] \tag{23}$$

The solution of this differential equation with appropriate boundary conditions at the sheath edge (on $\phi(r_s)$ and $\phi'(r_s)$) will yield the form of the potential and hence the electron density distribution inside the sheath(See below).However the equation is solved (eg., by iteration), there must be consistency with the Boltzmann approximation (Eqn (17) along with the quasineutrality assumption at the sheath edge which implies Eqn (21). These two constraints require that,

$$\exp(\frac{e\phi(r_1)}{T_e}) = (\frac{r_s}{r_1})^2[\frac{2\pi m}{M}]^{\frac{1}{2}} \tag{24}$$

Using these constraints and solving Eqn (23) by iteration we are able to produce an approximation to $\phi(r)$ as shown in Figure (1). (To produce a better rough approximation to the derivative, see the arguments related to the form of the presheath below).

Equation (24) applies for a capacitively coupled (floating) sphere only. If we apply a voltage to the sphere, its dc current I_{dc} becomes nonzero and Eqn (18) is no longer valid. That is, the electron velocity at r_s no longer can be equated to c_s but is instead given by

$$u_e(r_s) = c_s - \frac{I_{dc}}{4\pi r_s^2 e n_s} \tag{25}$$

The electron velocity at the sphere is still given by Eqn (19), however, and the Boltzmann relationship of Eqn (17) still holds. Consequently, conservation of electron flux now yields

$$r_s^2 u_e(r_s)=r_1^2(\frac{n_e(r_1)}{n_s})u_e(r_1)=r_1^2\exp[\frac{e\phi(r_1)}{T_e}][\frac{T_e}{2\pi m}]^{\frac{1}{2}} \tag{26}$$

Setting $c_s = (T_e/M)^{1/2}$ and using Eqn (25), we thus obtain

$$\exp[\frac{e\phi(r_1)}{T_e}]=[\frac{2\pi m}{M}]^{\frac{1}{2}}[(\frac{r_s}{r_1})^2-\frac{I_{dc}}{4\pi r_1^2 e n_s c_s}] \tag{27}$$

in place of the condition of Eqn (24). A negative external potential decreases the electron current reaching the sphere, so the net current I_{dc} becomes positive. Both the left-hand side and right-hand side therefore increase, and presumably r_s increases as well.

c. Presheath

In order to solve Eqn (23), even iteratively, it is necessary to apply boundary conditions on the function $\phi(r)$ in addition to its first derivative at the sheath edge as stated above. As an approximation to this a zero order estimate might be used which requires the potential to vanish along with its slope at this position. Although this yields an approximation to the solution for $\phi(r)$ and hence the electron density and plasma potential gradients, the solution strictly requires matching boundary conditions between the sheath and the presheath. Consequently we consider briefly the presheath model. To model the presheath, we assume the ions are collisionless as before but replace Poisson's equation with quasineutrality or,

$$n_e=n_+\equiv n \text{ for } r>r_s \tag{28}$$

We then use Eqns(16) and (17) to conclude that

$$\exp[\frac{e\phi}{T_e}][1-\frac{2e\phi}{T_e}]^{\frac{1}{2}}=[\frac{r_s}{r}]^2 \tag{29}$$

From this form we can obtain $\phi(r)$. The Eqn (29) has a solution which involves a Lambert function and for completeness this solution is shown in Figure (2) although we do not use the solution other than to note the asymptotic value of ϕ consistent with the requirement that the square root in Eqn (29) above must positive definite.

Three points are worth noting here. First, $\phi \geq 0$ in the presheath. Second, the voltage drop across the presheath is limited to $e\phi \leq 0.5\ T_e$. And third, the electric field in the presheath is given by

$$E = -\frac{d\phi}{dr} = -[\frac{r_s}{r}]^3[\frac{T_e}{er_s}][\frac{T_e}{e\phi}]\exp(-\frac{e\phi}{T_e})[1-\frac{2e\phi}{T_e}]^{\frac{1}{2}}. \qquad (30)$$

The field E in Eqn (30) points inward, as expected, but *diverges at* r_s where $\phi = 0$. The *divergence is unphysical but not unexpected, and it is in fact the basis for the Bohm condition,* $u+(rs) = c_s$. In reality quasineutrality fails before the Bohm condition is met, and thus a transition region is needed between the sheath and the presheath. Or what is the same thing, $E \rightarrow \infty$ at r_s from the presheath side but $E \rightarrow 0$ from the sheath side due to different scale parameters. This has been treated in some detail by Riemann for a sphere *[see p. 499 in J. Phys. D 24 (1991)]* . The point here is that we cannot use a boundary condition "exact" match from sheath to presheath. However, this is not really necessary for purposes here, as we are only interested in an approximate solution for $n_e(r)$ which will allow a calculation of the gradient in the sheath and hence the collisionless resistance.

V. Experimental Results and Comparisons to Theory

a. Collisionless impedance

It has been shown or demonstrated [4,18,23] that the complex impedance which arises for an alternating signal applied across an inhomogeneous plasma dielectric for parallel plate geometry of area A has a real part responsible for collisionless energy absorption which is given by,

$$R = \frac{\pi}{\epsilon_0 A \left| \frac{d\omega_{ep}(x)}{dx} \right|_{x=x_r}} \qquad (31)$$

(See Appendix III). This expression may be compared to Eqn (13) for the spherical case. It can be shown to be consistent with Eqn (13) after taking into account the difference between planar and spherical geometry and the inclusion of either two sheaths or one. In either case, if the driving signal frequency, ω, is outside the range of plasma frequencies inherent in the plasma dielectric, then R is not defined and the system response is purely reactive (i.e., the contour integral will have only a principal value contribution). If one then imagines the entire range of plasma frequencies of the inhomogeneous plasma to be a subset of a driving sweep, it might be concluded that the most energy will be deposited where $|d\omega_{pe}/dx|$, or $|d\omega_{pe}/dr|$ for the spherical case, has a local minimum. This is, however, not strictly true since R must be considered for the general case as a load resistor and viewed in light of its value with respect to the input impedance of the driving signal (ω) circuitry. Consequently the most efficient power transfer to the resistor (or the most energy absorption) does

not occur for R a maximum, but should occur at a frequency for which R is equal to the input impedance at resonance. At resonance the reactive part of the impedance is zero, the main plasma is collisionless and therefore R represents the effective impedance at resonance. As an example of this we note that in the limit of very large or very small R, there is no energy transfer as expected due to impedance mismatch, e.g., if the plasma considered is homogeneous, the gradient goes away and R = 0 consistent with no collisionless energy absorption. We plot in Figure (3) the experimental values of the $ReZ\,(R_\Omega)$ obtained for 3 different plasma densities as a function of ω/ω_{ps}; In Figure (4) we show once again experimental data, this time for Im Z, or the reactance. As expected the resistance shows a singularity at or near the bulk plasma frequency and low resistance, on the order of 100-200 Ohms near $\omega_{ps}/2$. This low resistive value is the closest to matching impedance with the Network Analyzer whose internal impedance is 50 Ω. (*We note here that data below will show significant power deposition at approximately this frequency.*) Also, the experimental reactance changes from capacitive to inductive behaviour, i.e, the reactance changes from capacitive to inductive reflecting the increase in the plasma component. Also, the reactance is negligible in the vicinty of $\omega_{ps}/2$. This must be the case if significant energy is to be transferred to the plasma impedance. In the next section we compare the absorbed power to data taken at different probe biases always, once again, in ion saturation. In a later paper we treat this case for electron saturation.

b. Observed energy absorption

We plot in Figure (5) the derived resistance of Eqn (13) based on the sheath density profile developed above for a bulk plasma density of $n_s = 2.5 \times 10^8\ cm^{-3}$. As noted above the resistance is closest to Network analyzer impedance approximately halfway into the sheath and this corresponds to an applied frequency near $\omega_{ps}/2$.

(i) Dependence on input signal strength

Shown in Figure (6) is a plot of reflected power at fixed density for the sphere in ion saturation at a DC bias level of V_{bias} = -5 Volts. Shown are three plots with varying input power from the network analyzer. The data is taken again for a plasma density of $2.5 \times 10^8\ cm^{-3}$ and a neutral pressure of $3.4 \times 10^{-4}\ Torr$. The abscissa of the plot is normalized driving frequency and the ordinate is normalized reflected power, $|\Gamma|^2$, (or $|S_{11}|^2$ as is the designation for the reflection coefficient). $|\Gamma|^2$ is defined as the ratio of reflected power, P_R, to total power, P_0, which includes also the reflected part and which is held constant by the instrument, or,

$$P_0 = P_R + P_T, \quad \textit{with} \quad |\Gamma|^2 = \frac{P_R}{P_0} \tag{35}$$

where P_T is the transmitted power. Clearly $1 - |\Gamma|^2$ is the normalized transmitted power, or the absorbed power, which depends upon the absorption mechanism. From these quantities then it is possible to calculate the impedance of the medium with which energy is exchanged or deposited. The

plots vary from an input voltage of 0.1 mV up to 10 mV. As can be seen from these data there is very little difference in reflected power as the input varies over a factor of 100. (We note here from these voltage levels and from the data that stochastic heating does not play a role in energy absorption levels.)

(ii) Dependence on bias voltage levels

We plot in Figure (7) an example of observed energy absorption at varying probe bias potentials for the case where the electron neutral collision frequency ,ν , is $4.5 \times 10^5\ s^{-1}$ corresponding to a neutral pressure of 2.5×10^{-4} Torr. In this case $\omega_p \sim 2 \times 10^3\ \nu$. The ordinate of the plot is the reflection coefficient defined above and we recall that $/S_{11}/^2$ is the normalized reflected power also as defined above. The energy absorption is seen to be a strong function of the bias level as would be expected if the resonance were a plasma sheath resonance. This result is shown more completely in Figure (8) where we show a contour plot of the power at each resonant frequency for varying bias voltages. In this 2D view, the relative intensity is used to indicate energy deposition as a function of frequency. As is expected, the resonance vanishes as the bias potential approaches the plasma potential and the sheath vanishes.

(iii) Energy absorption and required effective collision frequency

Figure (9) is an example of energy absorption observed for the small sphere compared to theoretical estimates for the case of no density gradient but increasing values of effective collision frequency in the main plasma.

The theoretical curves are plotted for 3 values of effective collision frequency all of which are at least two orders of magnitude higher than the actual collision frequency based on electron-neutral collisions. Also the calculation assumes no sheath and a constant density plasma using the impedance of Eqn (A3) in Appendix I below and the assumption of 50 ohm impedance matching between the cabling and the network analyzer. The unusual higher frequency oscillations in the data are associated with chamber resonances and are not part of the considerations related to absorption.

What is clear from this plot for our plasma conditions is that if we associate the apparent energy absorption seen with collisionless absorption, we must find the effective collision frequency much larger than the usual resistive component assumed responsible for the energy exchange. Below we have outlined an "effective resistance" which can be defined for this which is based on a plasma density gradient. In Figure (10) we plot the "effective"collision frequency based on the result of Eqn (A4) of Appendix A1 using collisionless resistance of Eqn (13) for R along with the derived sheath plasma density profile. It is seen that in the region of collisionless energy absorption(i.e., Figure (5) shows the closest approximation to impedance matching occurs around r = 1.1 cm), a required collision frequency near 6×10^7 sec $^{-1}$ is indicated consistent with Figure (9). Or, in the range of roughly 200 Ohms the collision frequency, ν , is seen in Figure (10) to be such that, $\nu \sim .01\text{-}.001\ \omega_p$, a collision frequency at least two orders of magnitude higher that due to Joule collisions and sufficient to produce detectable energy absorption phenomena.

(iv) Absorption as a function of Debye length

The series resonance shown in Figure (11) is a plot of the normalized frequency of the resonances observed as a function of Debye length, or plasma density. The data in Figure (11) were gotten by finding the maximum power absorption as a function of normalized frequency and then plotting versus a normalized probe radius. The plasma density was varied to produce the normalized probe radius. For example, the radius of the Aluminum sphere is on the order of 1 cm and for $\lambda_D \sim 0.05\ cm$, $n_e \sim 2.5 \times 10^8\ cm^{-3}$, and $R_p/\lambda_D \sim 20$ and, for this case, we are in the range where $R_p >> \lambda_D$. The theoretical curve (triangles) in Figure (11) are calculated using Eqn (36) below from an earlier work[11,19]. According to these calculations in the quasi-static approximation for monopole excitation of a sphere, the resonance positions are given approximately by,

$$\omega_r = \omega_{pe}\sqrt{\frac{s/R}{1+s/R}}, \tag{36}$$

where s is the sheath length. Further calculations using the Vlasov equation concluded that an approximation to s valid in many regimes is $s \sim 5\ \lambda_D$. This approximation is shown to be valid as long as R is not too small compared to λ_D. Using this value for s for the theoretical part of Figure (11), it appears that for our case the approximation is also a close one. The electron densities used in the calculation of λ_D were measured by a conventional Langmuir probe. The resonance frequencies, which were selected at the position of maximum energy absorption as described above, were taken without regard to the frequency width of the resonance and so there are no resolution estimates on the data. From Figure (7) it can be seen that the minima are well-defined. We conclude from this figure that the calculations based on sheath plasma resonance positions are consistent with the experimental data.

(v) Chamber radial density variation

Shown in Figure (12) is the plasma frequency, ω_{pe}, as a function of radial position taken from electron density measured by a Langmuir probe. Each data point is the average of a number of trials at a given radius and the spread in individual measurements is no greater than 10%. The position of the spherical probe was approximately at r = 0.1 m. It is clear from this figure that the density gradient in the main chamber plays no role in the collisionless absorption.

(vi) Magnetic field dependence

Finally for completeness we present data examining the effect of a magnetic field on the results. The presence of a magnetic field is expected to drastically alter the shape of the sheath with respect to the field direction in addition to a multitude of other possible effects[20] and therefore conclusions based on the field free case are not expected to hold in general. However, in order to maintain our plasma, it is necessary to apply a small axial (solenoidal) magnetic field on the order typically of ~ 2 Gauss. In fact the field introduces a preferred axis that alters the analysis, but the alterations are weak provided the electron cyclotron frequency is small compared to ω,

$$\Omega_e^2 \ll \omega^2. \tag{37}$$

In the experiments $\Omega e < 2 \times 10^8\ s^{-1}$ (for fields below 10 Gauss), whereas $\omega_{max} > 2 \times 10^8\ s^{-1}$ (for plasma densities above 10^7 cm-3). The condition of Eqn (37) is met for most all experimental conditions. To demonstrate this experimentally, shown in Figure (13) is a plot of the variation in resonance minimum as function of frequency and magnetic field varying from 1 to 10 Gauss. Although the range of variation of the magnetic field for this data is limited it nevertheless represents the actual range of magnetic field variation applicable in our experimental setup. Figure (14) is a plot of the maximum normalized positions of the resonance versus B as taken from Figure (13). Although there appears to be some effect discernible from the plot there is not a clear trend nor a dependence of peak position on magnetic field, at least for this data set in this limited range of B variation.

VI. Conclusions

We have observed collisionless energy absorption using a network analyzer for a small spherical probe in a vacuum chamber. We have used Maxwell's equations along with the continuity equation and assumptions on relative parameter magnitudes to calculate an effective collisionless resistance based on spherical geometry and a derived density profile. The resistance is evaluated as the residue of a contour integral consistent with earlier work. Sheath and presheath considerations have been taken into account to estimate the sheath electron density profile. We have estimated an effective collision frequency based on this resistance and find it to be on the order of two to three orders of magnitude higher than that due solely to Joule collisions. Our estimates of effective collision frequency are also experimentally based on results of measuring the reflected versus incident power to the probe using a network analyzer. As expected, the energy deposition vanishes in the limit of a vanishing sheath as a function of probe bias. Finally, there does not appear to be a magnetic field dependence for the low ranges of B necessary to maintain our plasma.

Acknowledgments: This work was supported by ONR

VII. Appendix I

An alternate widely-used elementary approach to an investigation of the effect of applying an *RF* field to a metallic object inside a vacuum chamber and immersed in a plasma is to assume that the configuration behaves approximately as a capacitor with a dielectric.[25,26] The boundaries are the conductor surface and the vacuum chamber walls. For an ordinary dielectric $C = C_0\, k$, with k the dielectric constant where $k>1$ and C_0 is the vacuum capacitance. For the plasma capacitor, $C = C_0\, \epsilon(\omega)$ where $\epsilon(\omega)$ is the dielectric constant. The straightforward estimate for $\epsilon(\omega)$ is based again on Maxwell's wave equations for a cold, non-drifting, unmagnetized plasma,

$$\nabla x(\nabla x \boldsymbol{E}) = -\frac{1}{c^2}\frac{\partial}{\partial t}(4\pi \boldsymbol{j} + \frac{\partial \boldsymbol{E}}{\partial t}) \equiv -\frac{1}{c^2}\frac{\partial^2}{\partial t^2}(\epsilon \boldsymbol{E}) \quad . \tag{A1}$$

Using the same assumptions for the electron momentum equation as in the main body of the text, we arrive at Eqn (8), and finally at the expression for the dielectric constant,

$$\epsilon(\omega) = 1 - i\frac{\omega_{pe}^{\,2}}{\omega(\nu + i\omega)} = \frac{\omega^2 + \nu^2 - \omega_{pe}^2}{\omega^2 + \nu^2} - i\frac{\nu\omega_{pe}^2}{\omega(\omega^2 + \nu^2)} \quad . \tag{A2}$$

Resistive effects are seen then to contribute via the imaginary part of $\epsilon(\omega)$. (The sign of this term is positive for an assumed $e^{-i\omega t}$ variation). Ion and neutral collisions both contribute to a collision frequency but the electron-neutral collision frequency is dominant over all other contributions under conditions of weak ionization or when $\nu / N < 10^{-3}$ where N is neutral gas density. In the experiment here we use an approximation to electron-neutral collision frequency as $\nu = 7 \times 10^{-8} N T_e^{1/2}$ and neutral pressure of 3 x 10^{-4} Torr ($N \sim 10^{13}\ cm^{-3}$). Electron density is typically on the order of 10^7-10^9 cm^{-3}.

It was noticed early on that if one uses the simple form for the permittivity in Eqn (A2), the impedance for a plasma capacitor, C, has the form of the impedance of a resistor and inductor connected in series, with both connected in parallel with a capacitor, C_0 , i.e., rearranging Eqn (A2) and substituting for C we have

$$Z = \frac{1}{i\omega C} = \frac{1}{i\omega \epsilon_r C_0} = \frac{1}{[i\omega C_0 + [\dfrac{\nu}{\omega_{pe}^2 C_0} + i\dfrac{\omega}{\omega_{pe}^2 C_0}]^{-1}]} \quad , \tag{A3}$$

where this familiar form of the impedance allows us by analogy to define the circuit inductance and resistance as[24,25]

$$L_p = \frac{1}{\omega_{pe}^2 C_0}, \quad R_p = \frac{\nu}{\omega_{pe}^2 C_0} = \nu L_p \ , \tag{A4}$$

where ω_{pe} is the plasma frequency. This idea leaves open the possibility of interpreting ν of Eqn (A4) loosely as an "effective" collision frequency in the absence of the usual resistive contribution. A radiation resistance, R_p, is then related to the plasma inductance as also seen in Eqn (A4).

The expression for the impedance given by Eqn. (A3) is not specific with respect to geometry and does not include a sheath between the probe/antenna and the plasma or between the plasma and the chamber walls. In addition we note that no provision has been made for an electron density gradient in the expression for plasma permittivity of Eqn (A2) which would render the analysis nonlinear. We can avoid the complications associated with the density gradient in the specific case of spherical geometry by considering a plasma-sphere system to consist of N concentric spheres of radius r_i, separated from one another by dielectric constants which vary as a function of radius but are constant between any two spheres. Using this assumption as the basis of the model the expression for total capacitance can be shown to be

$$\frac{1}{C_{total}} = \sum_{i=1}^{N} \frac{r_{i+1} - r_i}{\epsilon_i r_{i+1} r_i} \ . \tag{A5}$$

In the limit of small separation between the spheres this expression becomes the integral,

$$\frac{1}{C_{total}} = \int_{r_0}^{r_s} \frac{dr}{\epsilon_s(r) r^2} + \int_{r_s}^{r_c} \frac{dr}{\epsilon_p(r) r^2} \ , \tag{A6}$$

where r_c is chamber radius and we specifically separate the sheath region at the probe by integrating to the sheath edge and distinguish between permittivity in the sheath region, ϵ_s, and that in the main plasma, ϵ_p. We do not include a sheath at the large chamber walls. In this manner we introduce a plasma density which is a function of r in each region. Also, we recognize Eqn. (A6) as an alternate expression for the potential,

$$V(r_0) = -\left[\int_{r_0}^{r_s} E(r) dr + \int_{r_s}^{r_c} E(r) dr \right]. \tag{A7}$$

The total impedance now appears as

$$Z_{total}=\frac{1}{i\omega C_{total}}=\frac{1}{i\omega}\left[\int_{r_0}^{r_s}\frac{dr}{\epsilon_s(r)r^2}+\int_{r_s}^{r_c}\frac{dr}{\epsilon_p(r)r^2}\right]. \qquad \text{(A8)}$$

Substituting the result of Eqn (A2) for the collisionless case and collapsing the two integrals into one results in an identical expression to Eqn (10) in the main body of the paper.

The result for the collisionless resistance found in Eqn. (13) in the main body of the work is gotten by evaluating the integral for plasma impedance using a contour integral which separates the integral into a principal value integral in the upper-half complex plane plus the residue at the simple pole of the integrand. The residue at the pole provides a real contribution to the impedance which arises from the addition of the term $2\pi i\Sigma Res$ to the Cauchy principal value integral as described in that section. The integral to be evaluated derives from the expression of Eqn. (A8) and the definition of capacitance seen in Eqn (A6) or,

$$Z=\frac{1}{i\omega C}=i\omega\int_{r_0}^{r_s}\frac{\frac{dr}{\omega_p^2}}{r^2\left(1-\frac{\omega^2}{\omega_p^2}\right)} \qquad \text{(A9)}$$

where ϵ_s has been evaluated using Eqn (A2) with the collision frequency, $\nu = 0$. This expression is identical to Eqn (11) in the main body of the report. Appendix (II) below considers a widely-used and mathematically convenient form for the density profile in evaluating this integral; however, a more physically realistic model of the sheath profile is used to derive the results in the body of this work.

VIII. Appendix II

A commonly used expression for electron density spatial variation, employed often for mathematical ease in the case of planar geometry[4] is, in a spherical case with density increasing from *0* at r_0 , to n_s at the bulk plasma edge, r_s, given by,

$$n_e(r)=2n_s\ [1+\frac{s^2}{(r-r_0)^2}]^{-1} \tag{2A1}$$

where s, the sheath length, is r_s-r_0. If we require the sheath density gradient to have this form, the result for the real part of the complex impedance resulting from evaluation of the residue in the case of spherical geometry can be shown to be,

$$R(\omega)=\frac{\frac{\pi}{2}[\frac{2\omega_{ps}^2}{\omega^2}-1]}{(s+r_0[\frac{2\omega_{ps}^2}{\omega^2}-1]^{1/2})^2\ |\frac{d\omega_{ep}(r)}{dr}|_{r=r_r}} \tag{2A2}$$

In this form ω is the frequency corresponding to the plasma frequency at the resonant position, ω_{ps} is the maximum of the density profile occurring at the sheath edge (corresponding to n_s) for an applied bias in ion saturation, and ω_{pe} is the local plasma potential at r whose derivative is evaluated at the resonant position, r_r In this case,

$$|\frac{d\omega_{ep}(r)}{dr}|_{r=r_r}=\frac{\omega}{2s}\ [\frac{\omega^2}{\omega_{ps}^2}]\ [2\frac{\omega_{ps}^2}{\omega^2}-1]^{\frac{3}{2}} \tag{2A3}$$

where the pole in the integrand occurs at,

$$r_r=r_0+\ [\frac{2\omega_{ps}^2}{\omega^2}-1]^{-1/2} \tag{2A4}$$

We point out again, as in the main paper, that the collisionless resistance calculated arises not

from a bulk plasma density gradient but from a density gradient in the sheath at the probe itself.

IX. Appendix III

In a somewhat alternate approach appealing to energy consideration, power delivered to a parallel plate capacitor is compared to that absorbed to infer a collsionless resistance[18]. This association with resistance arises from first calculating the power absorbed by the plasma in a collisionless Vlasov calculation and comparing that to the power delivered. The expression for the power is a function of the parallel plate capacitor configuration and is not generally applicable to other geometries. The results are nevertheless useful as an alternate means of estimating R. The time-averaged power input into a parallel plate capacitor of area A, is shown to be[18]

$$\langle P\rangle = \frac{\pi\omega^2}{\left|\frac{d\omega_{pe}}{dx}\right|}\left(\epsilon_0\frac{\hat{E}^2}{2}\right) A, \tag{3A1}$$

where $j = i\omega\epsilon_0\hat{E}$ with $\hat{E}$ related to the perturbation electric field. and the derivative is taken at the resonant layer position. If we use this expression at the same time noticing that a plasma in general has both real current and displacement current and assume that the current very close to a plate surface is all displacement current (and is therefore the total current), the instantaneous power absorbed for the parallel plate geometry is given by

$$P = I^2R = \left(\epsilon_0\frac{\partial\Phi_E}{\partial t}\right)^2R \cong \epsilon_0^2\omega^2A^2\hat{E}^2R, \tag{3A2}$$

with the time averaged total power given as,

$$\langle P\rangle = \frac{1}{T}\int_0^T I^2R\,dt = \frac{1}{T}\int_0^T\left(\epsilon_0\frac{\partial\Phi_E}{\partial t}\right)^2R = \frac{\epsilon_0^2\omega^2A^2\hat{E}^2R}{2}. \tag{3A3}$$

Comparing Eqns (3A1) and (3A3), for the case of the cold, collisionless plasma slab, the effective resistive component appears as given in Eqn (31)[23].

X. References:

[1]Takayama, K., H. Ikegami and S. Miyazaki, Phys. Rev. Lett., **5**, 238 (1960)
[2]Uramoto, J.,Phys. Fl., **13(3)**, 657 (1970)
[3]Jackson, J.E. and J.A. Kane, J. Geophys. Res., **64(8)**, 1074 (1959)
[4]Ku, V.P.T., B.M. Annaratone, and J.E. Allen, J. Appl. Phys., **84**, 6536 (1998)
[5]Mishra, A., C.U.S. Patnaik, and P. Misra, J. Phys. Soc, Japan, **70**, 1966 (2001)
[6]Abdu, M.A., P. Muralkrishna I.S. Batista, and J.H.A. Sobral, J. Geophys. Res., **96**, 7689 (1991)
[7]Jensen, M.D. and K.D. Baker, J. Spacecraft and Rockets, **29**, 91 (1992)
[8]Balmain, K.G. IEEE Trans. Antennas Propagat., **605** (1964)
[9]Meyer, P., N. Vernet, and P. Lassudrie-Duchesne, J. Appl. Phys., **45(2)**, 700 (1974)
[10]Nikitin, P. And C. Swenson, IEEE Trans. Antennas Prop, **49(10)**, 1377 (2001)
[11]Harp, R.S. and F.W. Crawford, J. Appl. Phys., **35**, 3436 (1964)
[12]Dote, T. And T. Ichimiya, J. Appl. Phys., **36(6)**, 1866 (1964)
[13]Stenzel, R.L. Phys. Rev. Lett., **60(8)**, 704 (1988)
[14]Tonks, L., Phys. Rev. **37**, 1458 (1931)
[15]Herlofson, N., Arkiv. Fysik., **3**, 247 (1951)
[16]Barston, E.M., Ann. Phys.(N.Y.), **29**, 282 (1964)
[17]Buckley, R., Proc. R. Soc. London Ser. A **290**, 186 (1966)
[18]Crawford, F.W. and K.J. Harker, J. Plasma Phys., **8**, 261 (1972)
[19]Bekefi, G., **Radiation Processes in Plasmas**(Wiley, NY), Chapter 5 (1966)
[20]Bell, T.F. and T.N.C. Wang, IEEE Trans. Antennas and Propagation, **AP-19**, **4**, 517 (1971)
[21]Messiaen, A.M. and P.E. Vandenplas, Elec. Lett., **3**, 26 (1967)
[22]Ku, V.B.T.,PhD thesis, Oxford University (1996)
[23]Tanizuka, N and J.E. Allen, J Plasma Phys., **61**, 469 (1999)
[24]Lieberman, M.A. and A.J. **Lichtenberg, Principles of Plasma Discharges and materials Processing**, p303 ff, Wiley Interscience, New York, (1994)
[25]Blackwell, D.D., D.N. Walker, and W.E. Amatucci, Rev Sci Instrum, **76**, 023503 (2005)
[25a]Blackwell, D.D, D.N. Walker, S.J. Messer, W.E. Amatucci, Phys. Plasmas, (Accepted 7/21/05)
[26]Amatucci, W.E., D.N.. Walker, G.Ganguli, J.A. Antoniades, D. Duncan, and J.H. Bowles, Phys. Rev. Lett., **77**, 1978 (1996)
[27]Walker, D.N., D. Duncan, J.A. Stracka, J.H. Bowles, C.L. Siefring, M.M. Baumback and P. Rodriguez, Rev. Sci. Instrum, **65**, 661 (1994)
[28]Buneman, O., J. Appl. Phys., **32**, 1783 (1961)
[29]Chabert, P.,J.-L. Raimbault, J.-M. Rax and M. Lieberman, Phys. Of Plasmas, **11**, 1775(2004)
[30] Gozadinos, G. M.M. Turner, and D. Vender, Phys. Rev. Lett., **87**,135004(2001)
[31]Wang, T.N.C. and T.F. Bell, Radio Sci., **4(2)**, 167 (1969)
[32]Weenik, M.P.H., Radio Sci., **17**, 411 (1982)
[33]Riemann, K-U.,J. Phys. D, **24**, 493 (1991)

XI. Figures

Figure 1 Sheath potential (ϕ) vs distance from sphere (r) for sphere at floating potential

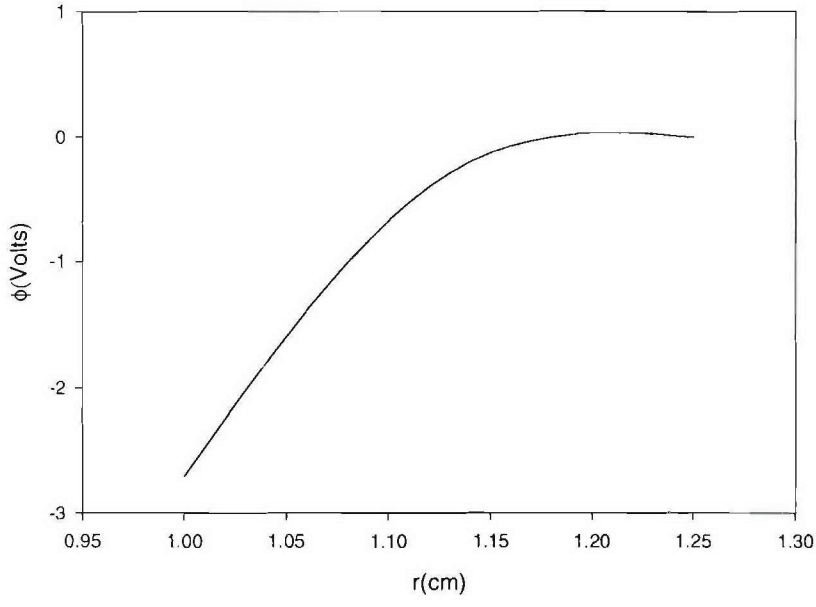

Figure 2: Presheath potential (ϕ) vs distance from sheath edge(r) for sphere at floating potential

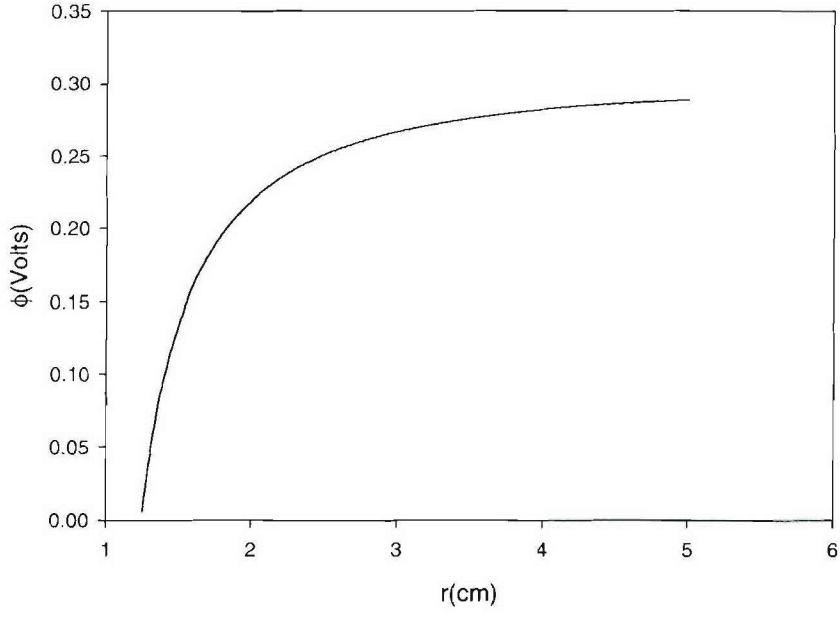

Figure 3: Measured resistance (R) vs applied frequency (ω):
(i) $n_e = 2.65 \times 10^7$ cm^{-3}, (ii) $n_e = 6.75 \times 10^7$ cm^{-3},
(iii) $n_e = 2.5 \times 10^8$ cm^{-3}

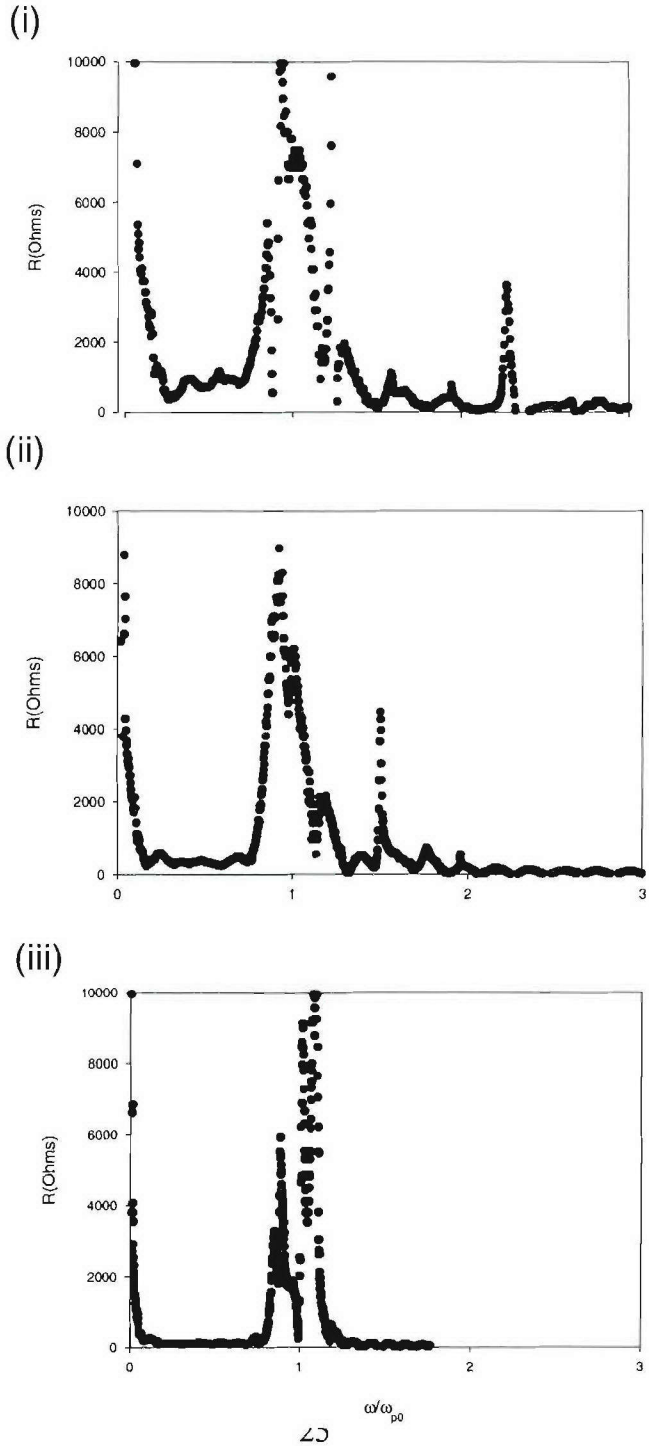

Figure 4: Measured reactance Im Z vs applied frequency (ω):
(i) $n_e = 2.65 \times 10^7$ cm^{-3}, (ii) $n_e = 6.75 \times 10^7$ cm^{-3},
(iii) $n_e = 2.5 \times 10^8$ cm^{-3}

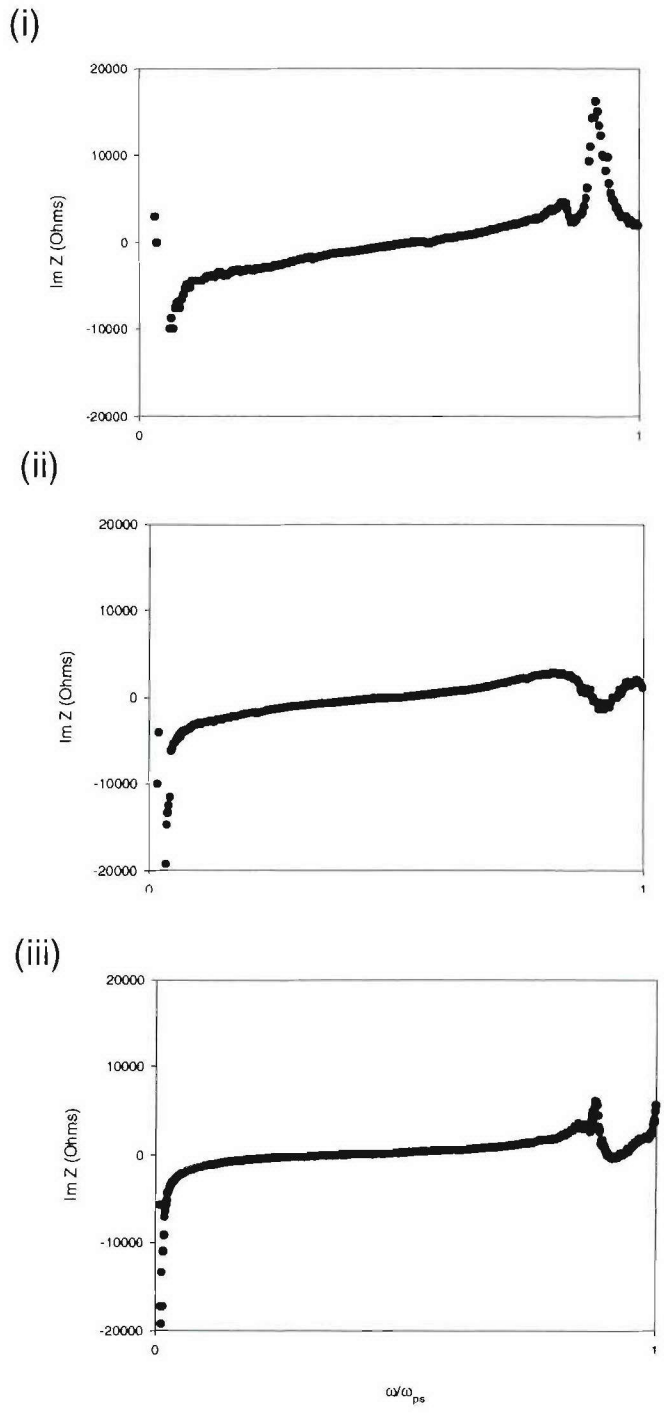

Figure 5: Collisionless resistance (R) vs radius (r) based on theoretical sheath model. Sheath edge at r=1.25 cm, sphere at r=1.0 cm

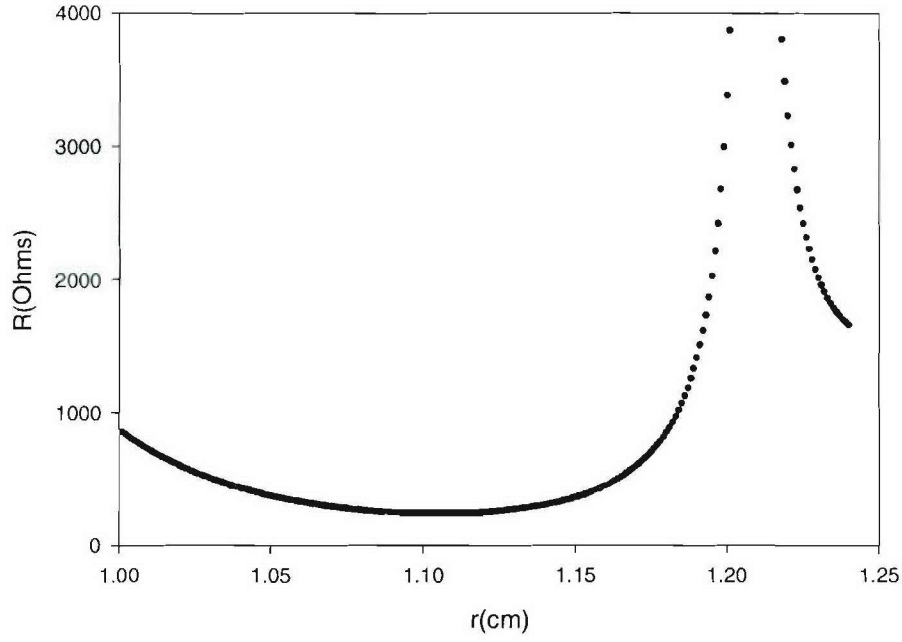

Figure 6: Reflected power (Γ^2) vs normalized frequency (ω/ω_{ps}) for 3 applied sweep voltage levels and a probe dc bias of -5 volts

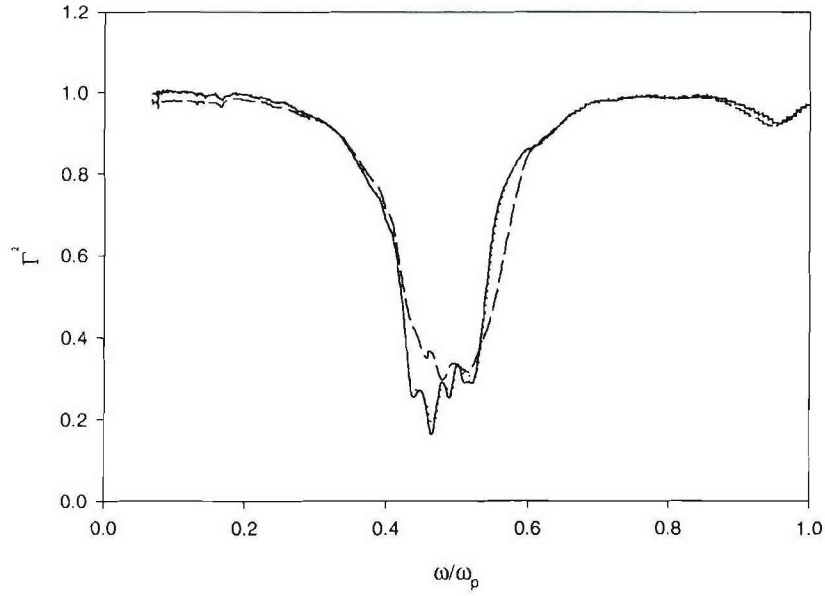

Figure 7: Energy absorption (|S11|) vs normalized applied frequency (ω/ωp) for differing probe dc bias levels.

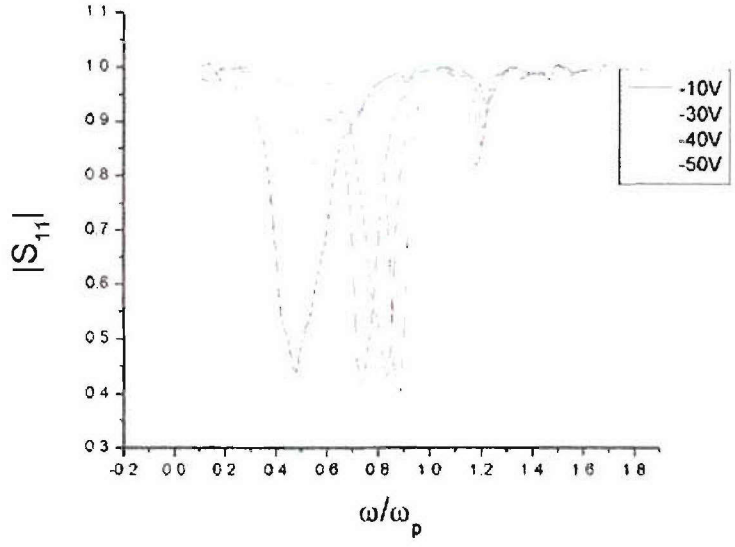

Figure 8: Contour plot of the power at each resonant frequency for varying bias voltages.

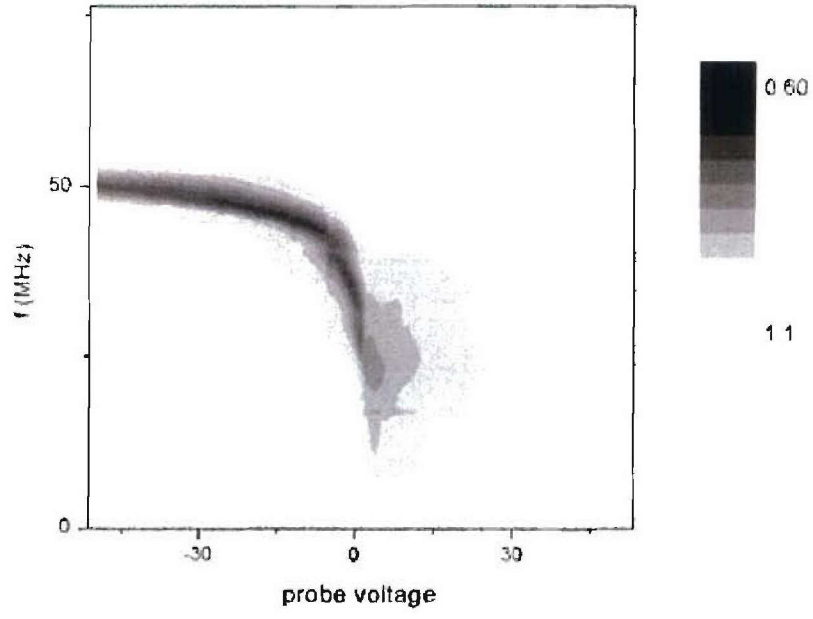

Figure 9: Normalized reflected power versus normalized applied frequency (ω/ω_p) for varying levels of collisions

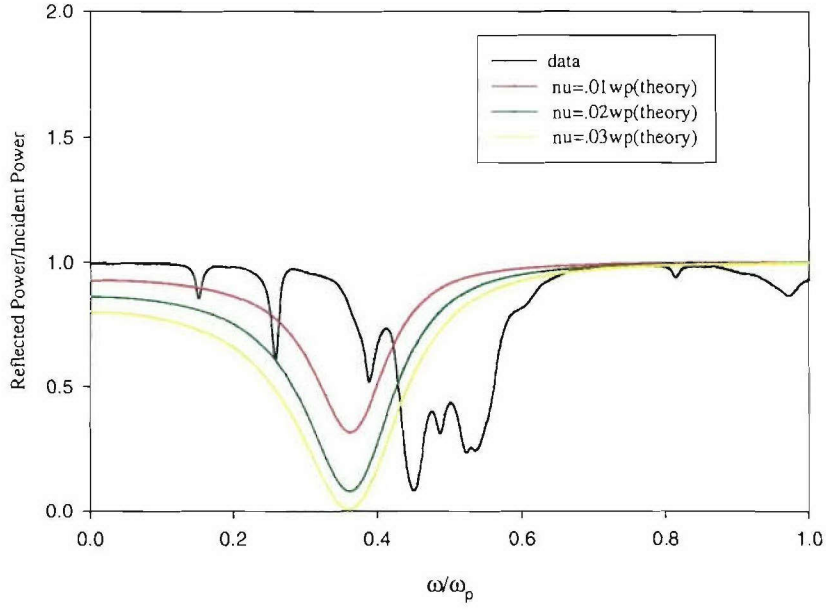

Figure 10: Effective Collision frequency (v) versus distance into sheath (r). Theoretical sheath model

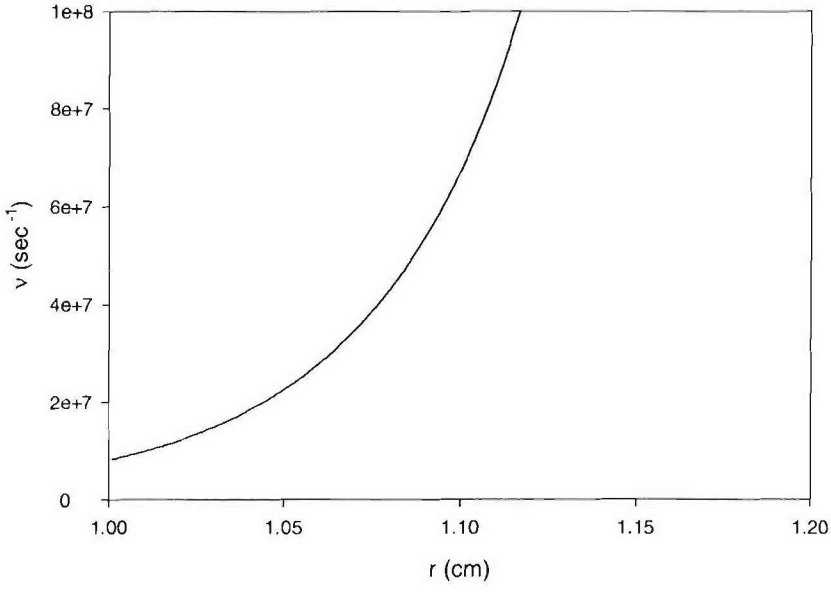

Figure 11: Normalized frequency of resonance (ω/ω_p) versus normalized sphere radius

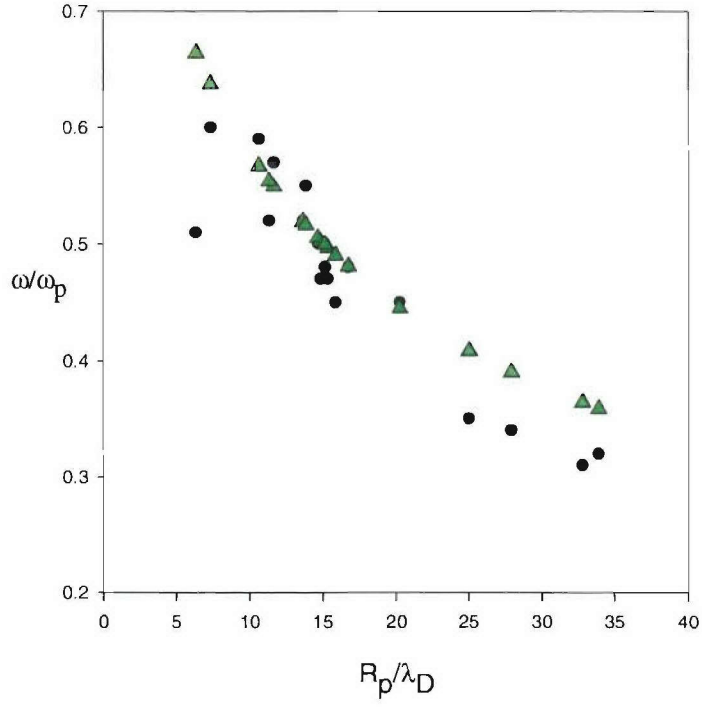

Figure 12: Bulk plasma frequency (ω_{ps}) versus radial distance from chamber center

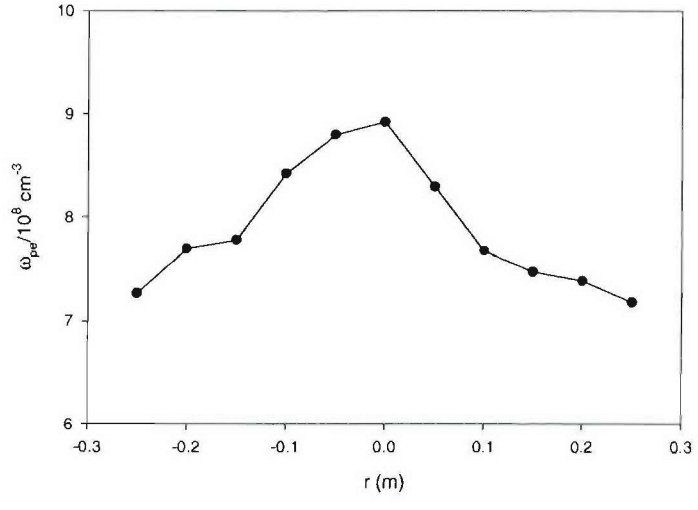

Figure 13: Variation in resonance minimum as function of magnetic field. Re (Γ) versus applied frequency (ω)

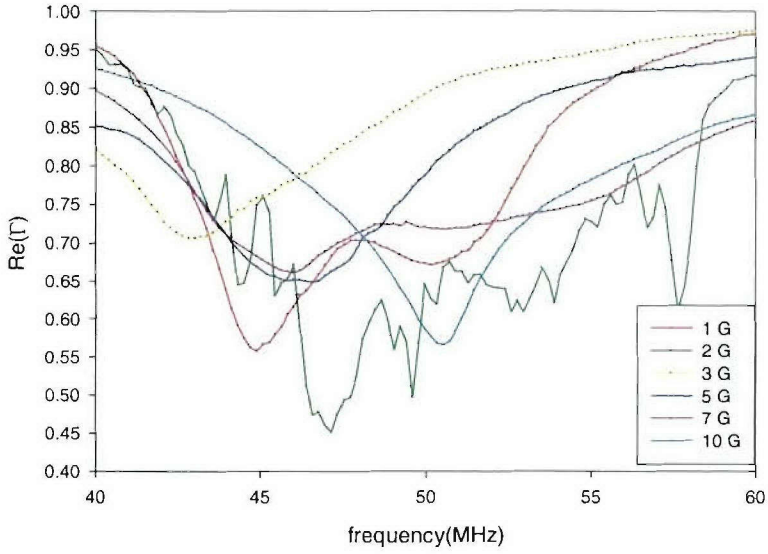

Figure 14: Normalized resonance minima positions (ω/ω_p) of Figure (12) versus B (Gauss)